PEEKWC Ultrafiltration Hollow-Fiber Membranes: Preparation, Morphology, and Transport Properties

F. Tasselli,[1] J. C. Jansen,[1] E. Drioli[1,2]

[1]*Institute on Membrane Technology (ITM-CNR), c/o University of Calabria, via P. Bucci, Cubo 17/C, 87030 Rende (CS), Italy*
[2]*Department of Chemical Engineering and Materials, University of Calabria, via P. Bucci, Cubo 17/C, 87030 Rende (CS), Italy*

Received 30 December 2002; accepted 25 April 2003

ABSTRACT: A series of hollow-fiber membranes was produced by the dry–wet spinning method from PEEKWC, a modified poly(ether ether ketone) with good mechanical, thermal, and chemical resistance. The fibers were prepared under different spinning conditions, varying the following spinning parameters: polymer concentration in the spinning solution, height of the air gap, and bore fluid composition. The effect of these parameters on the water permeability, the rejection of macromolecules (using dextrane with an average molecular weight of 68,800 g/mol), and the morphology of the membranes was studied. The results were also correlated to the viscosity of the spinning solution and to the ternary polymer/solvent/nonsolvent phase diagram. The morphology of the cross section and internal and external surfaces of the hollow fibers were analyzed using scanning electron microscopy (SEM). All membranes were shown to have a fingerlike void structure and a skin layer, depending on the spinning conditions, varying from (apparently) dense to porous. Pore size measurements by the bubble-point method showed maximum pore sizes ranging from 0.3 to 2 μm. Permeability varied from 300 to 1000 L/(h^{-1} m^{-2} bar) and rejection to the dextrane from 10 to 78%. The viscosity of polymer solutions was in the range of 0.2 to 3.5 Pa s. © 2003 Wiley Periodicals, Inc. J Appl Polym Sci 91: 841–853, 2004

Key words: poly(ether ether ketone); hollow-fiber membranes; phase separation; morphology; permeability

INTRODUCTION

Membrane-separation processes can nowadays be considered at the same level of importance as that of traditional unit operations. Their applications in almost all fields of research and industrial activities are widely consolidated.[1,2]

The always more particular needs of membranes to be used in chemically and/or physically aggressive environments drive scientists to develop new materials or modify existing ones. Synthetic polymeric materials offer the right answer to these needs for their capabilities of fitting specific requirements.

Some of these polymers, in spite of their excellent properties, cannot be used in the manufacturing of membranes by phase-separation processes because of their high crystallinity, making them almost insoluble in all solvents used in that technique.

Chemical modifications can sometimes render them useful for that purpose. For example, poly(ether ether ketone) (PEEK) polymers have very good chemical, mechanical, and thermal resistance but they are insoluble in the most common solvents except for strong concentrated acids. For that reason attempts have been made to modify these polymers[3] to make them more amorphous and soluble in common solvents.

Another completely different approach is the direct preparation of chemically modified polymers by the introduction of sterically cumbersome groups in the molecular chain. Zhang and Chou[4] patented a modified PEEK (PEEKWC, **Scheme 1**) obtained by polycondensation reaction between 4,4′-dichlorobenzophenone and phenolphthalein.

Among the great variety of polymers used in the preparation of membranes,[5] PEEKWC is one of the most recent and interesting. Its chemical, mechanical, and thermal characteristics[6] make it very competitive with other similar polymers. Its amorphous nature makes it well soluble in a variety of solvents,[3] both polar (NMP, DMF, DMA, THF) and nonpolar ($CHCl_3$, CH_2Cl_2, etc.). This allows the preparation of membranes by different procedures, such as solvent-induced phase separation (SIPS) and nonsolvent-induced phase separation (NIPS). Flat membranes of PEEKWC have already been prepared,[6,7] but not hollow fibers (HFs). The passage from flat membranes to HFs is neither simple nor immediate because of numerous parameters that play a prominent role in the formation of the latter type of membrane: for example, the geometry of the spinneret, the flow rate and the rheology of the polymeric solution inside the spinne-

Correspondence to: F. Tasselli (f.tasselli@itm.cnr.it).

Journal of Applied Polymer Science, Vol. 91, 841–853 (2004)

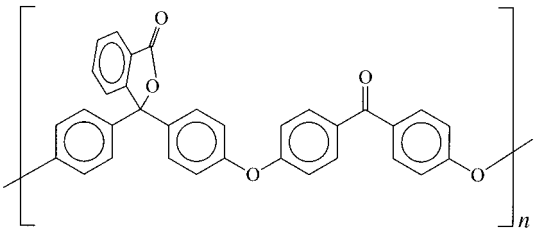

Scheme 1 Schematic representation of the structure of PEEKWC.

ret,[8] the flow rate of the internal coagulation fluid,[8,9] the presence of a double-coagulation process, the air gap,[8–11] and the take-up velocity.

In this study the preparation of HFs by the NIPS process and the influence of some of the above-mentioned parameters on the transport properties and the morphology of the membranes are discussed.

EXPERIMENTAL

Materials

PEEKWC, obtained from the Institute of Applied Chemistry, Changchun, China, was used as received without further treatment. *N,N*-Dimethylacetamide (DMA), an analytical reagent, was purchased from Lab Scan (Ireland). Dextrane (average molecular weight of 68,800 g/mol) was purchased from Fluka (Buchs, Switzerland). Glycerol was supplied by Carlo Erba Reagenti (Italy).

Preparation of the polymer solution

Solutions of PEEKWC at 12, 14, 16, 18, 20, and 23 wt % in DMA were prepared by slow addition of the polymer powder to the solvent under continuous mechanical stirring. The solution was stirred for 3 h and was then left standing for 2 h to remove air bubbles.

Phase diagrams

The ternary phase diagram of the system PEEKWC/DMA/water was determined by visual observation of the cloud point. Water was slowly added to the 15 wt % stirred polymer solution at ambient temperature (~ 20°C) until the solution became suddenly turbid. After registration of this first point, some extra water was added to cause precipitation of a significant amount of polymer. The mixture was then diluted with DMA until the solution became clear again (second point, "clearing point"). The entire procedure was repeated several times until the solution was too dilute to observe a turbidity change accurately.

Solution viscosity

The viscosity of PEEKWC solutions at concentrations of 12, 14, 16, 18, and 20 wt % in DMA was measured on a stress-controlled DSR 200 rheometer (Rheometric Scientific). The measurements were carried out at 25°C with the cone–plate configuration (cone and plate diameter 40 mm, gap 0.051 mm, cone angle 0.0399 rad) as a function of the shear rate.

Spinning method and apparatus

The polymer solution (dope) prepared as described above was loaded into the dope tank. The fibers were spun according to the dry–wet spinning process, using a spinning apparatus supplied by Stantech GmbH, Hamburg, Germany. The dope was forced through the spinneret by an N_2 overpressure and the flow rate was checked gravimetrically. The bore fluid was bidistilled water or its mixture with 25 or 50 wt % of DMA and it was fed to the spinneret by a metering pump. The flow rate of the dope and bore fluid were 12 and 15 g/min, respectively. Both the polymer solution and the bore fluid were kept at 30°C. The dope was filtered

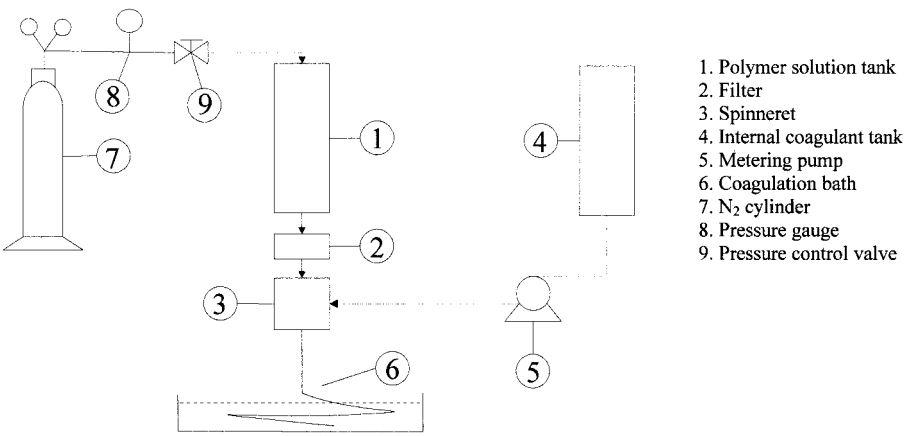

Figure 1 Schematic diagram of the apparatus for spinning of hollow fibers.

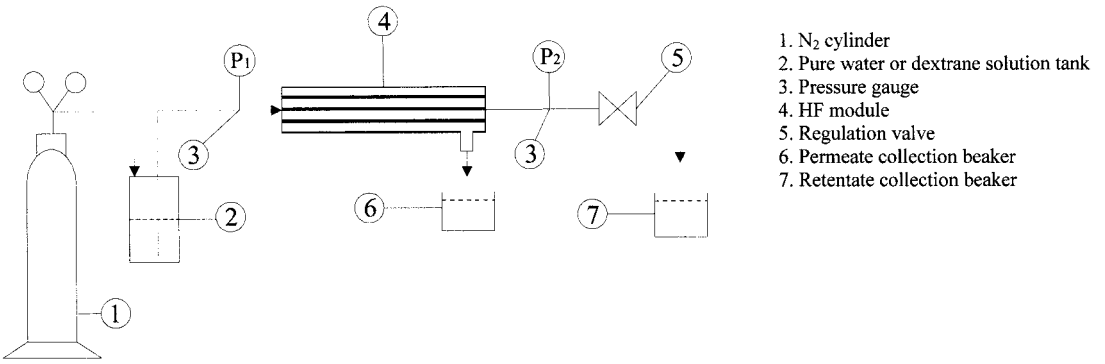

Figure 2 Schematic diagram of the apparatus for permeability and rejection measurements.

in line before entering the spinneret. The spinneret had a 2-mm hole and a needle for the bore fluid with an external diameter of 1 mm. The polymer solution leaving the spinneret entered an air gap that could be adjusted between 5 and 87 cm before dipping into the coagulation bath. In this rotating water bath the fibers were collected at the bottom and washed at the end of the spinning test. In Figure 1 a schematic diagram of the apparatus used for the spinning tests is shown.

Post-treatment

The spun fibers were cut in pieces of about 30 cm and kept in a fresh water bath for at least 24 h. Then they were soaked in a 20 wt % aqueous glycerol solution for 24 h and finally dried at room temperature for at least 2 days.

Permeability and rejection measurement

To measure permeability and rejection of macromolecules the fibers were mounted in a simple glass module (20 cm long) and fixed at both ends with epoxy resin. Water permeability was measured in a homemade setup by feeding bidistilled and filtered water (0.2-μm filter) by a nitrogen overpressure and weighing of the permeate stream. The transmembrane pressure (TMP) was regulated with a valve at the fiber outlet.

The apparatus consisted of a stainless steel water tank kept under N_2 pressure, a couple of manometers set at the inlet and the outlet of the module, and a regulation valve (Fig. 2).

The permeability P [in L/(h m bar)] was determined by measuring the volume of permeate (V_{permeate}) in a certain time (t) and at a certain transmembrane pressure.

$$P = V_{\text{permeate}}/(t \cdot A \cdot \text{TMP}) \quad (1)$$

where A is the membrane surface area. The average TMP over the length of the membrane is calculated as

$$\text{TMP} = (\Delta P_{\text{in}} + \Delta P_{\text{out}})/2 \quad (2)$$

TABLE I
Spinning Conditions and Dimensions of the Obtained Fibers[a]

Sample	PEEK WC concentration (wt %)	Bore fluid composition (% DMA in H_2O)	Air gap (cm)	ID (μm)	OD (μm)
1	12	0	5	1040	1540
2	14	0	5	1154	1634
3	16	0	25	1012	1508
4	16	25	25	1164	1554
5	16	50	25	1359	1772
6	18	0	12	1078	1600
7	18	0	25	1000	1484
8	18	0	50	980	1455
9	18	0	87	887	1355
10	20	0	50	988	1550
11	20	25	50	1173	1573
12	20	50	50	1273	1591
13	23	0	50	1073	1682

[a] Other conditions: dope flow rate 12 g/min; bore fluid (BF) flow rate 15 g/min.

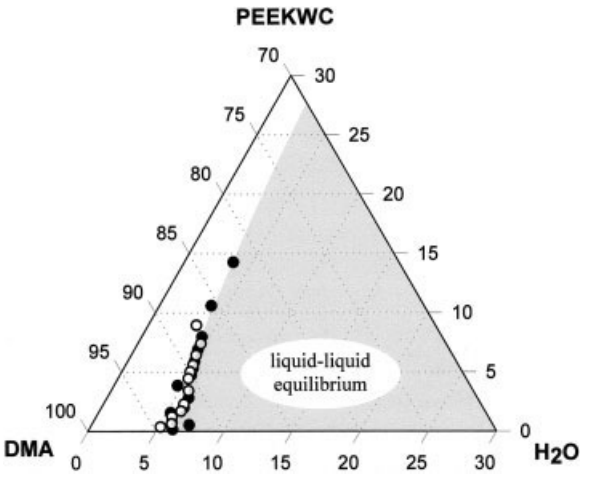

Figure 3 Ternary phase diagram of the system PEEKWC/DMA/water at ambient temperature, determined by cloud point measurement. Solid symbols indicate the clear–turbid transition upon addition of water; open symbols indicate the turbid–clear transition upon addition of DMA.

where ΔP_{in} and ΔP_{out} are the differences between feed and permeate pressure at the inlet and outlet of the module, respectively. Rejection of macromolecules was determined by means of a solution of dextrane with an average molecular weight of 68,800 g/mol. The dextrane was dissolved in bidistilled water at a concentration of 0.2 g/L. The procedure and the apparatus for feeding the dextrane solution were the same as those used for the water permeability measurements. After 1 h from the beginning of the test, samples of the mother solution and permeate were collected and analyzed. The dextrane concentration was determined according to a spectrophotometric method.[12] The rejection R was calculated as

$$R = 100(C_F - C_P)/C_F \tag{3}$$

where C_F and C_P are the concentration of the dextrane in the feed and permeate solution, respectively.

Pore size determination

The maximum pore size was measured by the bubble-point method in a simple self-constructed setup.[13] A fiber was mounted with epoxy resin in an open-ended module to form a loop. The fiber was then filled with water and the module was connected to a compressed air cylinder and immersed in water. The pressure was gradually increased with about 100 mbar/min until the first air bubble column appeared.

Determination of the overall porosity

The overall porosity was calculated according to the following equation:

$$\varepsilon = 100\% \times \left(1 - \frac{\text{Density}_{\text{fiber}}}{\text{Density}_{\text{PEEKWC}}}\right)$$

in which the fiber density was calculated from its mass and volume according to

$$\text{Density}_{\text{fiber}} = \frac{4m}{\pi(OD^2 - ID^2)l}$$

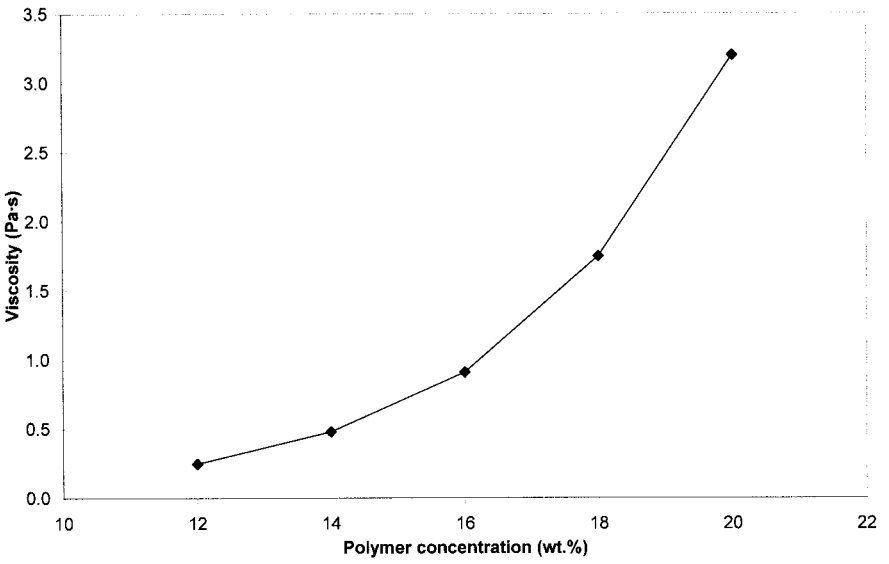

Figure 4 Viscosity of the PEEKWC solution in DMA as a function of the polymer concentration at a constant shear rate of 1 s^{-1}.

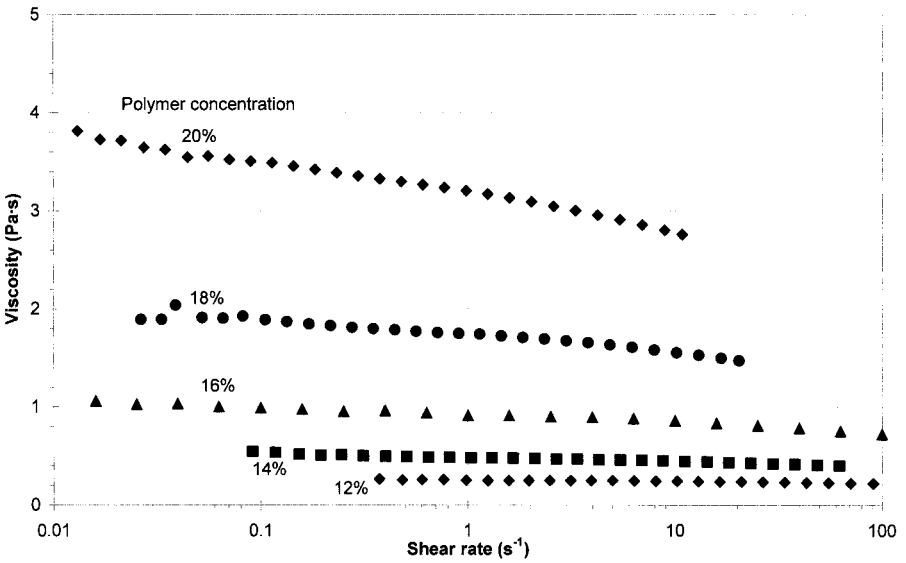

Figure 5 Viscosity of the PEEKWC solutions in DMA as a function of the polymer concentration and the shear rate.

where l is the length of the fiber sample, m is its mass, and ID and OD are the inner and outer diameter, respectively. The density of PEEKWC is 1.24 g/cm^3.

Scanning electron microscopy (SEM)

The membrane morphology was studied by SEM (Cambridge Stereoscan 360). HF samples were freeze fractured, using liquid N_2 to produce a clean brittle fracture, and were subsequently sputter-coated with gold before SEM observation.

RESULTS AND DISCUSSION

A series of fibers was produced under different operating conditions, varying polymer concentration, bore fluid composition, and air gap.

Table I reports the operating conditions and their influence on the inner and outer diameter (ID and OD) of the produced fibers.

Phase diagram

The phase diagram is shown in Figure 3. The binodal demixing curve was determined by visual observation of the cloud point during nonsolvent addition to the clear polymer solution and by solvent addition to a partially demixed solution. With increasing polymer concentration the binodal demixing curve moves closer to the PEEKWC-DMA axis, indicating that demixing occurs at increasingly small amounts of water. The maximum polymer concentration used for the present procedure was limited to about 15 wt %. At very low polymer concentration observation of turbidity changes becomes more difficult, resulting in some scatter in the data points.

Viscosity of the polymer solutions

The phase-separation process during membrane formation is a complex mix of thermodynamic and ki-

TABLE II
Influence of the Dope Concentration on the Fiber Dimensions and Bubble Point Pore Size[a]

Sample	PEEK WC concentration (wt %)	Air gap (cm)	ID (μm)	OD (μm)	Pore size (μm)
1	12	5	1040	1540	2
2	14	5	1154	1634	1
3	16	25	1012	1508	0.7
7	18	25	1000	1484	0.4
10	20	50	988	1550	0.3
13	23	50	1073	1682	0.3

[a] Other conditions: BF pure water; BF flow rate 15 g/min; dope flow rate 12 g/min.

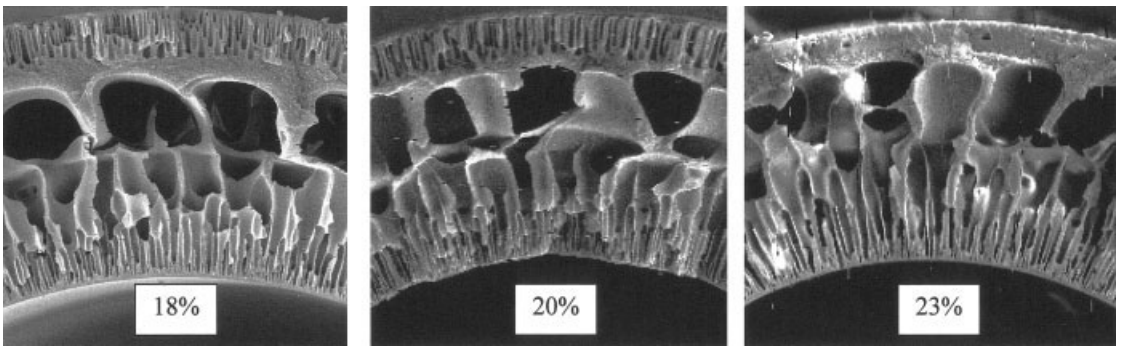

Figure 6 Cross sections (detail) of HF obtained from dopes at different polymer concentrations.

netic phenomena. One of the main parameters influencing the kinetics of the phase inversion is the viscosity of the polymer solution. Therefore the viscosity of the PEEKWC/DMA solution was measured as a function of polymer concentration. The results are shown in Figure 4.

The viscoelastic properties of the polymer solution are also important for the spinning process. The shear rates generated in the spinneret might have an influence on the morphology and on the final transport properties of the membranes. Therefore the viscosity of the polymer solutions was also measured as a function of the shear rate. The results are displayed in Figure 5. With increasing polymer concentration the viscosity strongly increases and it becomes shear-rate dependent. Especially at a polymer concentration of 20 wt % the solution is clearly shear thinning, even at shear rates as low as 0.01 s^{-1}. This indicates that some orientation of the dissolved polymer chains may occur during the spinning process.

For the flow of Newtonian fluids through an annular tube, the shear rate is highest at the inner wall of the annulus and it is given by

$$\gamma_R = \frac{4Q_s}{\pi R^3}\left(\frac{k\log(1/k) - (1-k^2)/2k}{(1-k^4)\log(1/k) - (1-k^2)^2}\right) \qquad (4)$$

in which γ_R is the shear rate at the inner wall, Q_s is the flow rate, R is the outer diameter of the annulus, and k is the ratio of the inner diameter and outer diameter of the annulus.[8]

For our setup, with inner and outer diameters of the spinneret of 1 and 2 mm, respectively, $k = 0.5$ and eq. (4) reduces to $\gamma_R = 340.4Q_s$ (Q_s in cm^3/s). At a typical flow rate of 12 mL/min the maximum shear rate is thus $\gamma_R = 340.4 \times (12/60) = 68.1\ s^{-1}$. At this value the PEEKWC solutions with the highest concentrations clearly demonstrate shear thinning behavior. In reality the maximum shear rate will be even higher than

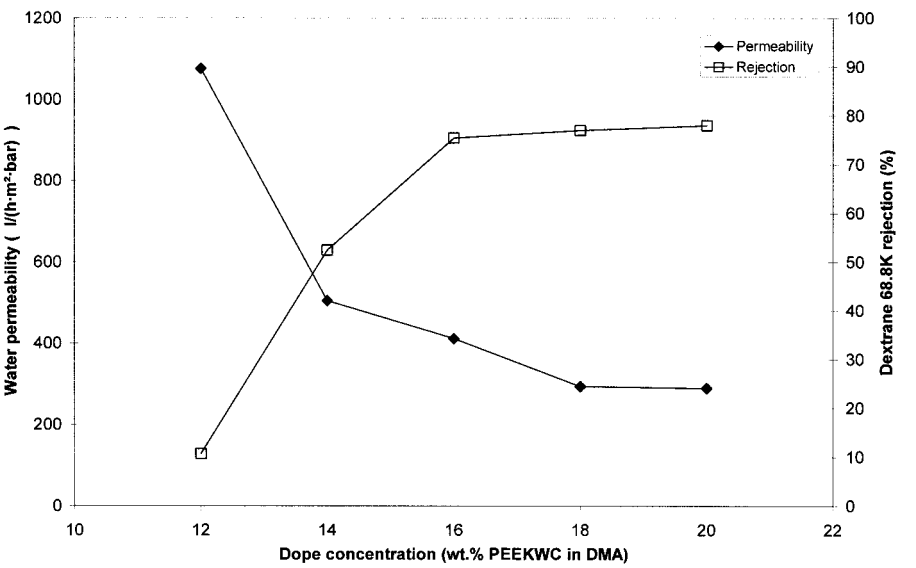

Figure 7 Effect of the dope composition on the water permeability and dextrane rejection.

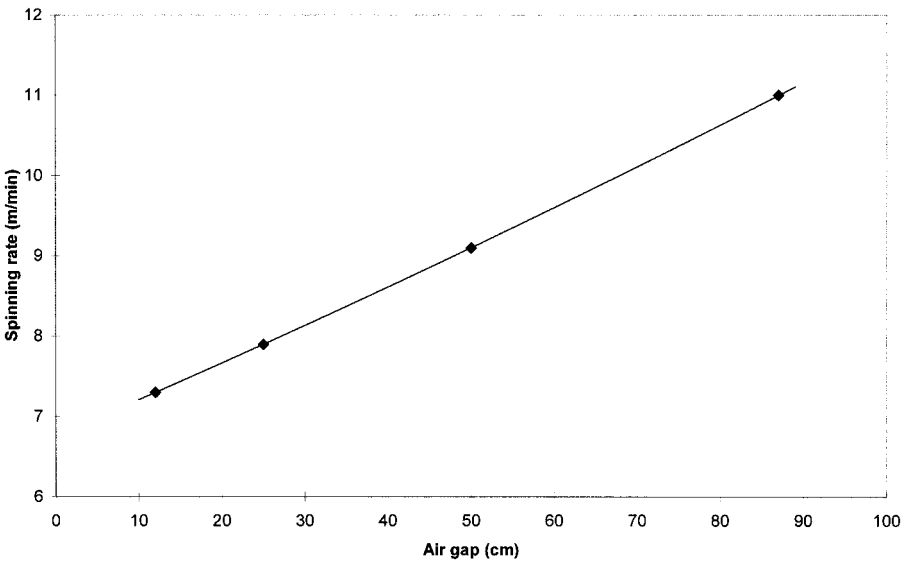

Figure 8 Dependency of the spinning rate on the air gap.

calculated for the Newtonian liquid above, given that shear thinning fluids tend to have a plug flow profile, resulting in higher shear rates at the wall. Therefore it is likely that some orientation of the polymer chains occurs inside the spinneret. If the subsequent relaxation is sufficiently slow, the orientation may be partly frozen in upon precipitation of the polymer in the coagulation bath or upon contact with the bore fluid. This might have some influence on the morphology and/or transport properties of the membranes.[8] However, this phenomenon was not studied in detail in the present work because the dope flow rate was kept constant in all experiments. In addition it would be difficult to distinguish exactly the effect of the chain orientation because the shear rate also influences other parameters such as the membrane thickness.

Influence of the dope composition

The polymer concentration in the dope was varied from 12 to 23 wt %. As seen above, the viscosity of the solution is strongly dependent on the polymer concentration. The range of concentration was chosen for practical reasons: below 12% the solution becomes so liquid that no stable jet is formed outside the spinneret and above 23% the solution is too viscous to be pumped with acceptable speed with the present setup.

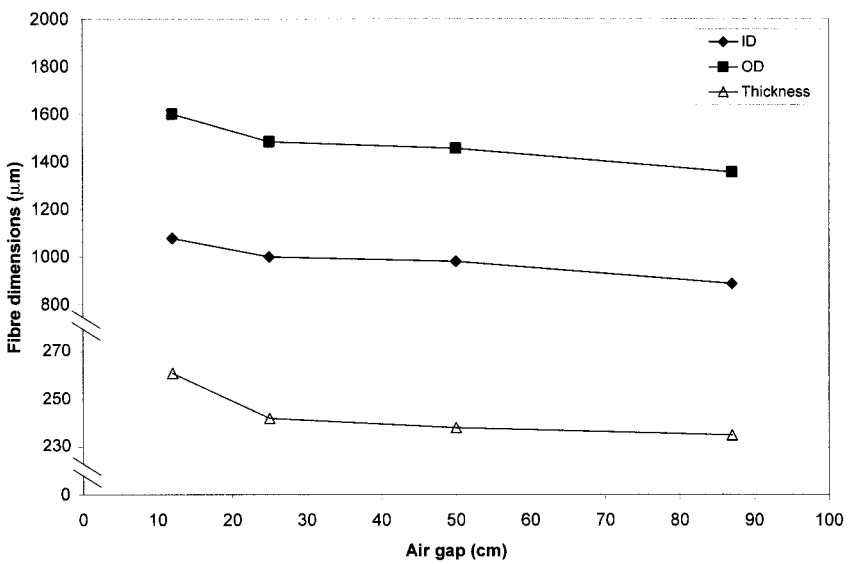

Figure 9 Inner diameter, outer diameter, and membrane thickness as a function of the air gap.

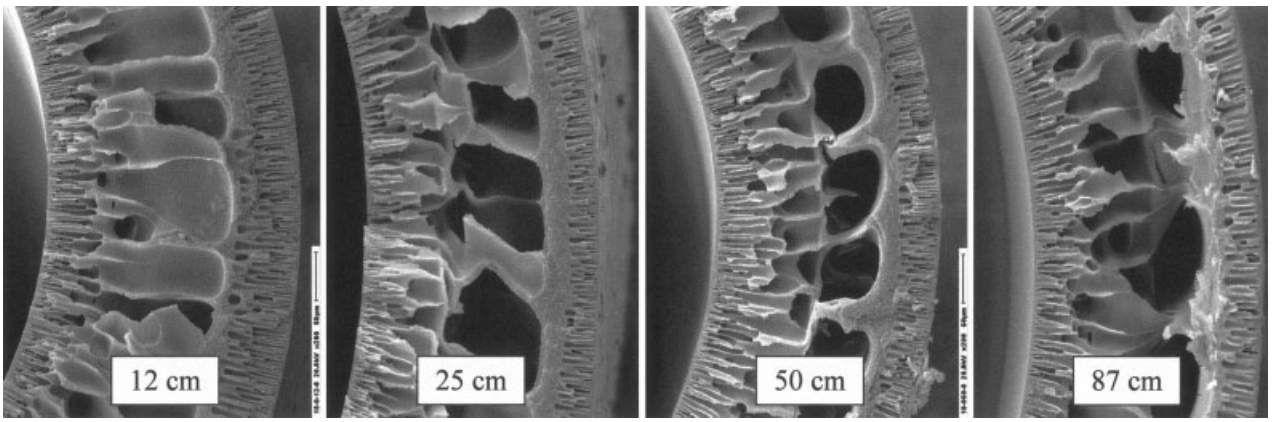

Figure 10 SEM image of the cross section of fibers prepared with different air gaps (details).

An overview of the experimental conditions and the obtained fiber dimensions is listed in Table II.

The air gap was varied to keep the spinning rate and fiber dimensions more or less constant. This operation is justified because the air gap has relatively little influence on the membrane permeability (see below). Although an increase in the air gap *reduces* the dextrane rejection, this effect is negligible compared to the strong *increase* of the dextrane rejection caused by the increase of the polymer concentration.

Among the principal effects induced by the variation of the polymer concentration in the dope, the most important are the variation of the morphology and transport properties of the formed membrane. Figure 6 shows the cross section of some HFs obtained from dopes with different polymer concentrations.

As may be observed they present a similar structure with a double layer of fingerlike voids. The external layer becomes increasingly dense and compact when the dope concentration increases and with a dope concentration of 23% the external layer is almost free of voids. This is in good agreement with the findings of Kesting et al.[14] who reported the formation of a double fingerlike void structure with a polysulfone dope at 17%, whereas only at 37% of polymer did they obtain a structure completely free of fingerlike voids.

Close examination of the fibers shows that the morphology changes cannot be a result of the polymer concentration alone, given that the increase of the polymer concentration in the dope solution mainly affects the morphology of the outside of the fiber and not of the inside. The most likely explanation finds its origin in the phase diagram (Fig. 3). In the short interval that the fiber passes through the air gap (about 4 s) it may absorb a small amount of humidity from the air. This brings the solution closer to demixing conditions. It is well known that addition of nonsolvent to the casting solution tends to suppress the formation of macrovoids.[13] Indeed this is most likely to occur in a more concentrated PEEKWC solution because the binodal demixing curve moves closer to the DMA–PEEKWC axis (lower water concentrations) at relatively high PEEKWC concentrations.

On the other hand, at the bore side of the fiber the contact with water is always immediate, thus triggering more or less the same demixing process, leading to more or less the same morphology.

The water permeability and dextrane rejection of the membrane in their turn are strongly influenced by the variation of the polymer concentration in the dope. The first decreases whereas the second increases when the polymer concentration increases in the spinning solution. As may be seen from Figure 7, P decreases from more than 1000 to about 300 L/(h m bar) and the rejection of the dextrane 68,800 g/mol increases from 11 to 78%.

Furthermore, bubble-point measurements suggest that the pore size (see Table II) is also influenced by the polymer concentration in the dope. The pore size trend fits well with that of the permeability and rejection: the higher the pore size, the higher the permeability and the lower the rejection. This is a natural consequence of the more "dense" structure of external layer of the fibers, as discussed above (Fig. 6).

Influence of the air gap

The influence of the air gap on the performance and morphology of hollow fibers has often been investigated and discussed.[8–11] The air gap influences basically all the main characteristics of the hollow-fiber membranes: the fiber dimensions, morphology, and transport properties. Figure 8 shows the influence of the air gap on the spinning rate.

The increase of the air gap implies the increase of the length of the nascent fiber suspended from the spinneret. This causes a higher stretching of the emerging dope attributed to the gravitational force, resulting in an elongation of the nascent fiber and, as

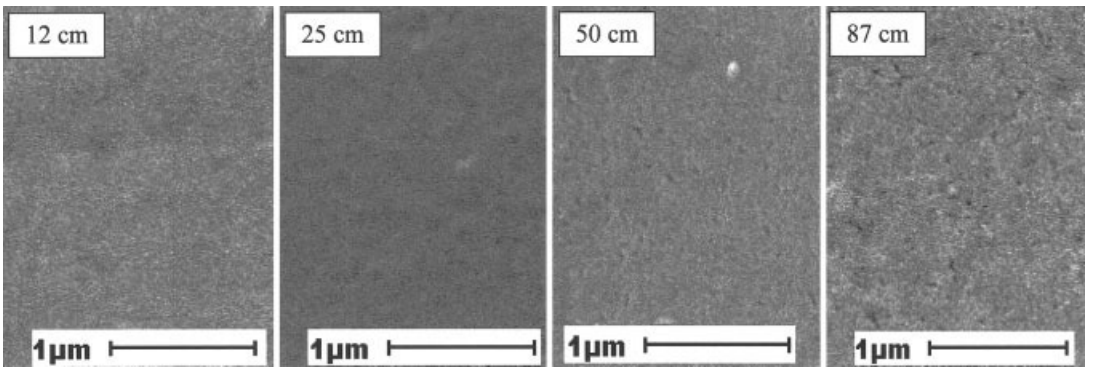

Figure 11 Effect of the air gap on the HF structure (outer surfaces).

a consequence, in a higher spinning rate. One of the effects of a higher spinning rate is the reduction of the fiber dimensions. Figure 9 shows the dependency of the ID, OD, and membrane thickness on the air gap and hence on the spinning rate.

As may be seen the OD, ID, and thickness decrease proportionally when the air gap increases, as confirmed by the OD/ID ratio that remains almost constant. This is a result of the longitudinal stretching of the fiber by gravitational force.

SEM observation of the cross sections shows that the air gap apparently has no significant influence on the overall morphology on a macroscopic scale (see cross sections in Fig. 10). However, the outer surface, upon closer observation, shows an increasing number of pores or microfractures in the range of 0.1–0.3 μm (Fig. 11).

Moreover, the dextrane rejection decreases drastically with increasing air gap (Fig. 12), suggesting that the pore size in the inner surface increases as well. This may be a result of the elongation of the nascent membrane under the gravitational force and a disruption of the thin surface layer. However, the actual pore size ($\ll$100 nm) is too small to observe any significant differences between the four samples by SEM. The water permeability does not vary appreciably, probably because the water flux through the membrane is controlled by the overall porosity that remains almost unchanged: 79 $\pm$ 2% without a particular trend. Thus, to improve the selectivity without compromising the permeability the air gap should be kept as small as possible yet sufficiently high to guarantee an acceptable spinning rate (Fig. 8).

Influence of the bore fluid (BF) composition

In the present work, two sets of experiments were carried out to investigate the influence of the BF composition on the characteristics and performances of the produced fibers.

Table III reports these two sets of fibers and other information that will now be discussed; Figure 13

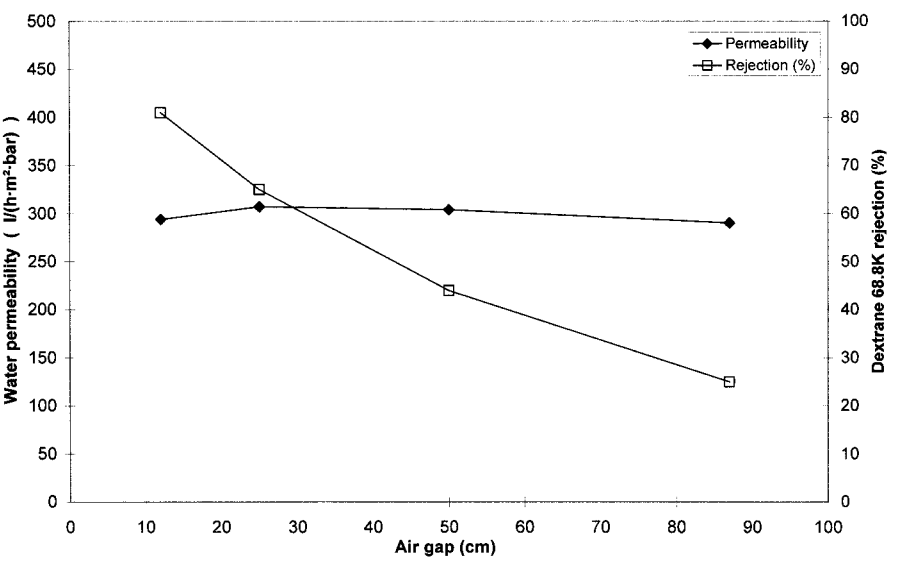

Figure 12 Permeability and dextrane rejection as a function of the air gap.

TABLE III
Influence of the Bore Fluid Composition on the Fiber Dimensions[a]

Sample	PEEK WC conc. (wt %)	Bore fluid (% DMA in H_2O)	Air gap (cm)	ID (μm)	OD (μm)	OD/ID
3	16	0	25	1012	1508	1.49
4	16	25	25	1164	1554	1.33
5	16	50	25	1359	1772	1.30
10	20	0	50	988	1550	1.57
11	20	25	50	1173	1573	1.34
12	20	50	50	1273	1591	1.25

[a] Other conditions: dope flow rate 12 g/min; BF flow rate 15 g/min.

shows the cross sections and the inner surface of the fibers belonging to the first set and Figure 14 shows the influence of the bore fluid composition on the transport properties.

As may be observed, all characteristics of the fiber are strongly influenced by the variation of BF composition. This can be ascribed to various reasons: hollow-fiber formation is a complex process involving several different phenomena, such as die swelling[15] attributed to the dope flow rate, extension attributed to gravity or to an external drive, swelling arising from the bore fluid flow rate, compaction attributed to coagulation, transport of solvent and nonsolvent through the fiber, and thermodynamics and kinetics of the phase-separation process itself. Which factor is most important depends on the specific experimental conditions.

If we look at the fiber dimensions we find that both the inner and the outer diameters increase whereas the membrane thickness decreases with increasing solvent concentration in the bore fluid. This can be ascribed mainly to the inflation of the fiber caused by the much higher flux of the bore fluid than that of the dope solution. The degree of inflation, and hence the fiber dimensions, depends on the bore fluid composition through the mechanical strength of the fiber: a strong coagulant like pure water instantaneously creates a rigid polymer skin that is difficult to inflate, whereas a poor coagulant like the 50/50 DMA/water mixture leads to a delayed onset of liquid–liquid demixing and hence a slower gelation (see below), allowing a stronger inflation of the fiber. It is interesting to notice that an increase of both the inner and the outer diameters corresponds to a decrease in the membrane thickness, in contrast to what occurs on variation of the air gap, where an increase of fiber diameter is always accompanied by an increase of the membrane thickness (see above). This is mainly a result of the stretching of the membrane film, predominantly in the longitudinal direction in the case of the air gap variation, and in the axial direction in the case of the bore fluid variation. Both lead to a thinner film, but the former leads to a lower fiber diameter and the latter to a higher fiber diameter.

From a practical point of view the possibility to control the fiber dimensions is very important because it allows improvement of the mechanical resistance through the thickness, or the filtrating area through the diameter.

In addition to the macroscopic fiber dimensions, the morphology is also influenced by the bore fluid composition. As one of the effects, Figure 13 shows the change from an almost compact surface layer to one with a discrete pore distribution of appreciable dimensions. For flat membranes it is known that delayed onset of demixing tends to produce nonporous membranes with a thick and dense top layer while at the same time a lower polymer concentration at the interface of the nascent film, caused by the increase of solvent in the BF, leads to a more open skin layer.[13] In the case of hollow-fiber formation these two contrasting effects are further complicated by the fact that a lower polymer concentration in the interface reduces the resistance of the forming film to mechanical stresses, thus increasing the stretching of the nascent fiber by the gravitational force.

The effect of the BF composition on the phase inversion is indicated qualitatively in the phase diagram of the PEEKWC/DMA/water system (Fig. 15). The diagram shows a series of (imaginary) concentration paths for a 20 wt % polymeric solution (black square) in contact with water with an increasing DMA concentration. The effect of increasing solvent concentration is indicated with an arrow. As a result of the lower nonsolvent concentration in the coagulant, the concentration paths "penetrate" less deeply into the metastable/unstable biphasic region and also the equilibrium composition of the polymer-rich phase moves along the binodal demixing curve toward higher DMA concentration and lower polymer concentration (black dots). At the same time the diffusive flux of the nonsolvent decreases with increasing DMA concentration in the bore fluid, increasing the time scale in which the entire process of phase inversion takes place, resulting in delayed onset of demixing. At very high DMA content in the bore fluid, the film does not develop significant mechanical resistance before reaching the rotating external coagulation bath and a very irregularly shaped film is formed because of mechanical deformation (Fig. 16).

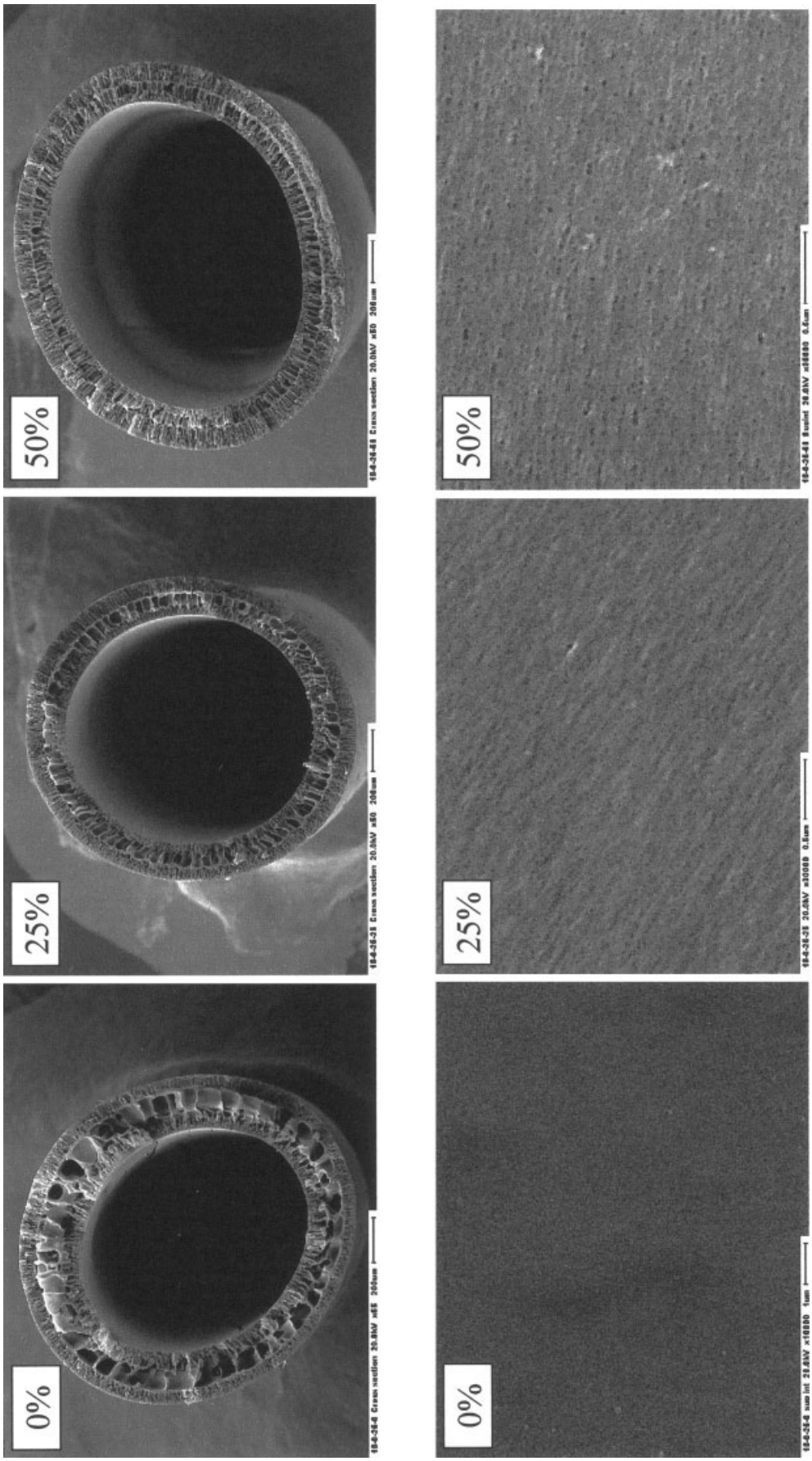

Figure 13 Effect of the bore fluid composition (% DMA in water) on the fiber dimensions and morphology with a dope at 16% of polymer.

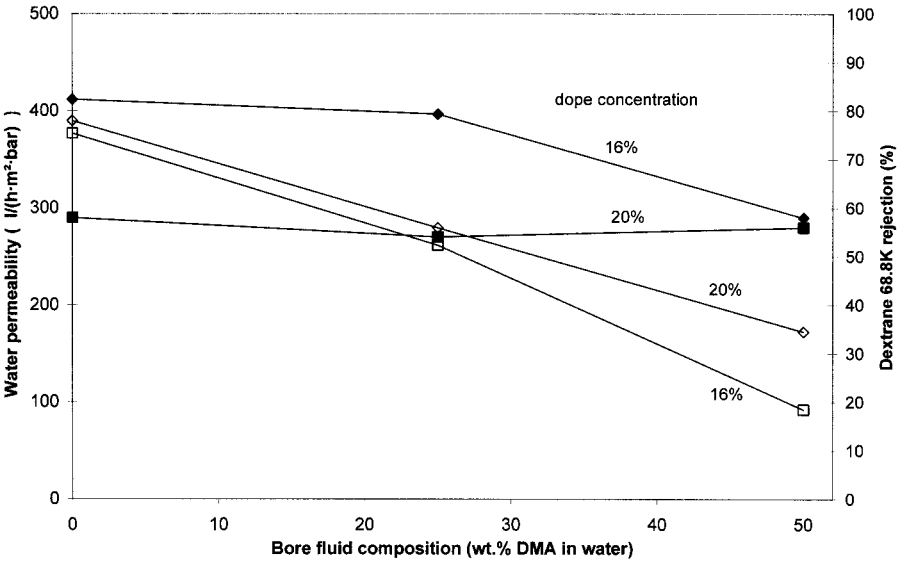

Figure 14 Water permeability (solid symbols) and rejection of 68,800 MW dextrane (open symbols) as a function of bore fluid composition and dope concentration.

In the literature the influence of the bore fluid composition was investigated by several authors,[16–21] sometimes leading to opposing conclusions. For polysulfone gas-separation membranes Pesek and Koros[16] reported that the selectivity increased when the water activity was lower in the bore fluid, although Shieh and Chung did not find a significant difference in permeance and selectivity with their cellulose acetate gas-separation membranes spun with different bore fluid compositions. For polysulfone ultrafiltration membranes Doi and Hamanaka[20] and Chau et al.[21] found that the solute rejection decreased when they used bore fluids with reduced water activity. This is in good agreement with our own results for the PEEKWC UF membranes (Fig. 14). It is possible to conclude that the results depend strongly on the type of membranes (dense GS membranes or porous UF membranes) and on the specific experimental conditions (i.e., the combination polymer/solvent/nonsolvent, the flow rate of the polymer solution, the internal coagulant, etc.). For our specific system the overall result of the increase of the DMA concentration in the bore fluid is the observed change in fiber dimensions and morphology, the reduction of the dextrane rejection and a more or less constant water flux.

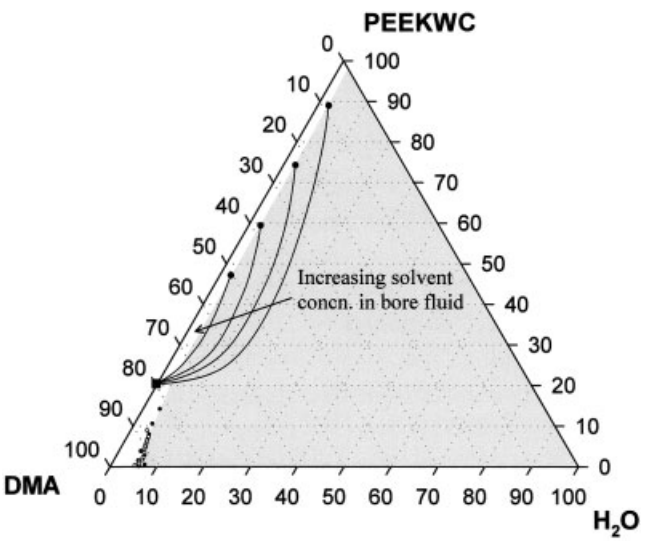

Figure 15 Influence of the bore fluid composition on the phase-separation process: a qualitative sketch* of the concentration paths of the film/BF interface for increasing DMA concentration in the bore fluid. [*Concentration paths and extrapolation of the bimodal demixing curve to high polymer concentration are not based on experimental data but serve only as a visual guide to the explanation of the observed phenomena.]

CONCLUSIONS

In this study it has been demonstrated that PEEKWC can be used successfully in the manufacturing of hollow-fiber membranes for UF applications.

The characteristics of the hollow fibers produced under different operating conditions (polymer concentration, air gap, and bore fluid composition) demonstrate the possibility of preparing customized membranes. An increase in the polymer concentration in the dope allows a simultaneous increase of macromolecule rejection and decrease of the permeability, whereas a change in the bore fluid composition allows an improvement of the rejection, independent of the water flux. The specific surface area can be controlled by proper adjustment of the air gap and the solvent content in the bore fluid, both having the same effect on the film thickness but the opposite effect on the

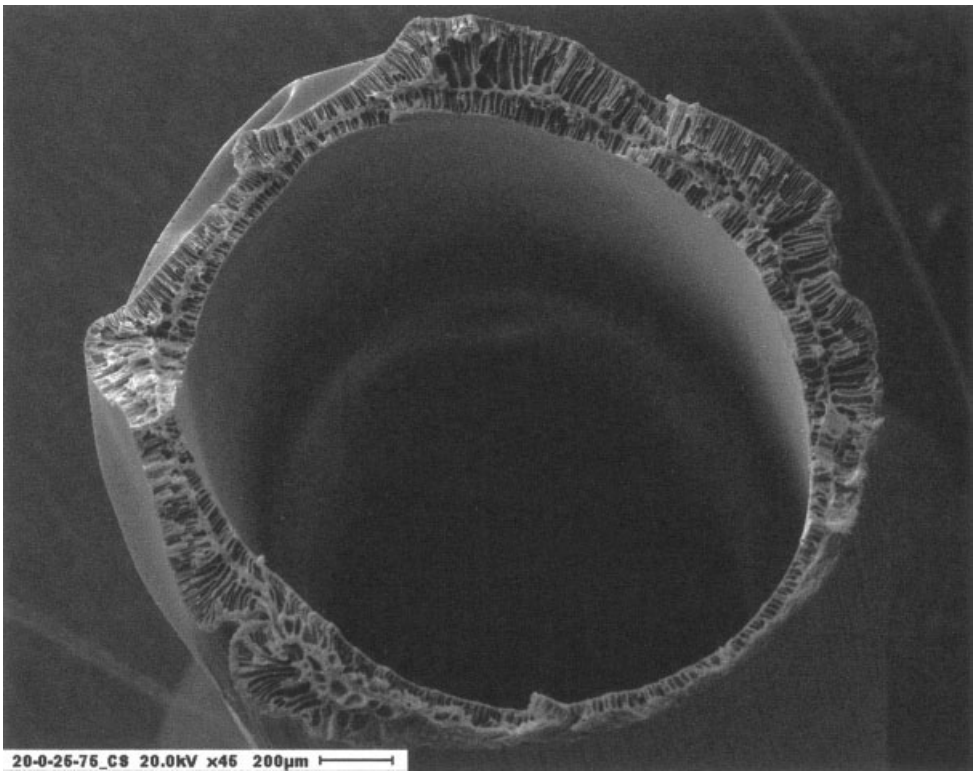

Figure 16 Fiber prepared from a 20% dope and 75/25 DMA/H_2O mixture as the bore fluid.

fiber diameter. The morphology (e.g., pore size, absence/presence of macrovoids and fingers) can be controlled by the dope concentration and to a lesser extent by the composition of the bore fluid.

The authors thank the colleagues of the Institute of Applied Chemistry of Changchun, China for kindly supplying the PEEKWC polymer, and Dr. M. Davoli of the University of Calabria, Rende, Italy for carrying out the SEM analysis.

References

1. Drioli, E.; Romano, M. Ind Eng Chem Res 2001, 40, 1277.
2. Cassano, A.; Molinari, R.; Romano, M.; Drioli, E. J Membr Sci 2001, 181, 111.
3. Trotta, F.; Drioli, E.; Moraglio, G.; Baima Poma, E. J Appl Polym Sci 1998, 70, 477.
4. Zhang, H.; Chen, T. Chin. Pat. 85108751 (1987).
5. Kesting, R. E. Synthetic Polymeric Membranes; Wiley: Irvine, CA, 1985.
6. Drioli, E.; Zhang, H. Chimica oggi 1989, November, 59.
7. Buonomenna, M. G.; Figoli, A.; Jansen, J. C.; Davoli, M.; Drioli, E. In: Membranes Preparation, Properties and Applications, Proceedings of the MRS Boston Fall Meeting 2002; Burganos, V. N.; Noble, R. D.; Asaeda, M.; Ayral, A.; LeRoux, J. D., Eds.; Vol. 752, to appear.
8. Aptel, P.; Abidine, N.; Ivaldi, F.; Lafaille, J. P. J Membr Sci 1985, 22, 199.
9. Miao, X.; Sourirajan, S.; Zhang, H.; Lau, W. Y. Sep Sci Technol 1996, 31, 141.
10. Chung, T.; Hu, X. J Appl Polym Sci 1997, 66, 1067.
11. Chung, T. J Membr Sci 1997, 126, 19.
12. Dubois, M.; Gilles, K. A.; Hamilton, J. K.; Rebers, P. A.; Smith, F. Anal Chem 1956, 28, 350.
13. Mulder, M. Basic Principles of Membrane Technology; Kluwer Academic: Dordrecht, 1991.
14. Kesting, R. E.; Frietzsche, A. K. Polymeric Gas Separation Membranes; Wiley: New York, 1993.
15. Ziabicki, A. Fundamentals of Fiber Formation; Wiley: New York, 1976.
16. Pesek, S. C.; Koros, W. J. J Membr Sci 1994, 88, 1.
17. Sharpe, I. D.; Ismail, A. F.; Shilton, S. J. Sep Purif Technol 1999, 17, 101.
18. Idris, A.; Ismail, A. F.; Noordin, M. Y.; Shilton, S. J. J Membr Sci 2002, 205, 223.
19. Shieh, J. J.; Chung, T. S. J Membr Sci 1998, 140, 67.
20. Doi, S.; Hamanaka, K. Desalination 1991, 80, 167.
21. Chau, J. L.; Wang, S. S.; Guo, C. L. Ind Chem Res 1995, 34, 803.